NMRF / RR / 07/2024

RESEARCH REPORT

Assessment of Wind Forecasts from NWP Model for Indian NPP Sites

Priya Singh, Sushant Kumar, Raghavendra Ashrit

May 2024

National Centre for Medium Range Weather Forecasting

Ministry of Earth Sciences, Government of India

Assessment of Wind Forecasts from NWP Model for Indian NPP Sites

Priya Singh, Sushant Kumar, Raghavendra Ashrit

National Centre for Medium Range Weather Forecasting

Ministry of Earth Sciences

A-50, Sector 62, NOIDA-201309, INDIA

May 2024

1	Name of the Institute	National Centre for Medium Range Weather Forecasting (NCMRWF)
2	Document Number	*NMRF/RR/07/2024*
3	Date of publication	May 2024
4	Title of the document	Assessment of Wind Forecasts from NWP model for Indian NPP Sites
5	Type of Document	Research Report
6	No. of pages & Figures	34 Pages &18 Figures
7	Number of References	21
8	Author (S)	Priya Singh, Sushant Kumar, Raghavendra Ashrit
9	Originating Unit	NCMRWF
10	Abstract	The purpose of a Decision Support System (DSS) for nuclear emergencies is to furnish emergency managers with thorough and timely information regarding situations arising from a nuclear accident. The DSS integrates various elements, including the released source term, meteorological conditions, dispersion and deposition in the environment, and calculates the affected areas, population exposure, and the impact of protective actions on potential dose. The accuracy of Numerical Weather Prediction (NWP) data is among the factors influencing the forecast of public dose. This report evaluates the performance of NCMRWF Unified Model-Global (NCUM-G), for wind speed and direction forecasts at nine selected Indian Nuclear Power Plant (NPP) sites. The study has been performed considering the measured and predicted hourly winds for the year 2023. Forecast accuracy is evaluated using standard statistical methods used for linear and circular variables. The performance of the model in forecasting wind speed and direction has been systematically evaluated on both annual, seasonal and

		temporal scales. The measured and predicted wind data is found to be in good convergence, though the distribution of individual differences between measured and predicted wind data indicated random error. Additionally, the study also assesses the effectiveness of bias correction, leading to improved wind speed forecasting, particularly at the NPP sites with higher forecast errors.
11	Security classification	Non-Secure
12	Distribution	Unrestricted Distribution
13	Key Words	Nuclear Power Plant, NWP Model, Nuclear Emergency, Surface winds, Wind Forecasts, Bias Correction

Table of Contents

Assessment of Wind Forecasts from NWP Model for Indian NPP Sites

Priya Singh, Sushant Kumar, Raghavendra Ashrit

सारांश

परमाणु आपात स्थितियों के लिए निर्णय समर्थन प्रणाली (डीएसएस) का उद्देश्य आपातकालीन प्रबंधकों को परमाणु दुर्घटना से उत्पन्न स्थितियों के बारे में संपूर्ण और समय पर जानकारी प्रदान करना है। डीएसएस विभिन्न घटकों जैसे, उत्सर्जित तत्वों एवं उनका पर्यावरण में फैलाव और जमाव, मौसम समन्धित स्थितियां, जनसंख्या जोखिम और संभावित क्षेत्र पर सुरक्षात्मक कार्यों के प्रभाव की गणना करता है। संख्यात्मक मौसम पूर्वानुमान (एनडब्ल्यूपी) डेटा की सटीकता सार्वजनिक मात्रा के पूर्वानुमान को प्रभावित करने वाले कारकों में से एक है। यह रिपोर्ट नौ चयनित भारतीय परमाणु ऊर्जा संयंत्र (एनपीपी) स्थलों पर हवा की गति और दिशा के पूर्वानुमान के लिए एनसीएमआरडब्ल्यूएफ यूनिफाइड मॉडल-ग्लोबल (एनसीयूएम-जी) के प्रदर्शन का मूल्यांकन करती है। यह अध्ययन वर्ष 2023 के लिए अवलोकित तथा मॉडल पूर्वानुमानित हवाओं को ध्यान में रखते हुए किया गया है। पूर्वानुमान सटीकता का मूल्यांकन रैखिक और परिपत्र चर के लिए उपयोग की जाने वाली मानक सांख्यिकीय विधियों का उपयोग करके किया जाता है। हवा की गति और दिशा के पूर्वानुमान में मॉडल के प्रदर्शन का वार्षिक, मौसमी और समयांतरालिक पैमानों पर व्यवस्थित रूप से मूल्यांकन किया गया है। प्रथम दृष्टया में अवलोकित तथा मॉडल पूर्वानुमानित पवन डेटा अच्छे अभिसरण में पाए गए हैं, हालांकि इनके बीच व्यक्तिगत अंतर के वितरण ने यादृच्छिक त्रुटि का संकेत दिया है। इसके अतिरिक्त, यह अध्ययन विशेष रूप से उच्च पूर्वानुमान त्रुटियों वाले एनपीपी साइटों पर पूर्वाग्रह सुधार की प्रभावशीलता का भी आकलन करता है, जिससे हवा की गति के पूर्वानुमान में सुधार हो।

कीवर्ड: परमाणु ऊर्जा संयंत्र, एनडब्ल्यूपी मॉडल, परमाणु आपातकाल, सतही हवाएं, हवा का पूर्वानुमान, पूर्वानुमान त्रुटि सुधार

Abstract

The purpose of a Decision Support System (DSS) for nuclear emergencies is to furnish emergency managers with thorough and timely information regarding situations arising from a nuclear accident. The DSS integrates various elements, including the released source term, meteorological conditions, dispersion and deposition in the environment, and calculates the affected areas, population exposure, and the impact of protective actions on potential dose. The accuracy of Numerical Weather Prediction (NWP) data is among the factors influencing the forecast of public dose. This report evaluates the performance of NCMRWF Unified Model-Global (NCUM-G), for wind speed and direction forecasts at nine selected Indian Nuclear Power Plant (NPP) sites. The study has been performed considering the measured and predicted hourly winds for the year 2023. Forecast accuracy is evaluated using standard statistical methods used for linear and circular variables. The performance of the model in forecasting wind speed and direction has been systematically evaluated on both annual, seasonal and temporal scales. The measured and predicted wind data is found to be in good convergence, though the distribution of individual differences between measured and predicted wind data indicated random error. Additionally, the study also assesses the effectiveness of bias correction, leading to improved wind speed forecasting, particularly at the NPP sites with higher forecast errors.

Keywords: Nuclear Power Plant, NWP Model, Nuclear Emergency, Surface winds, Wind Forecasts, Bias Correction

1. Introduction:

A Decision Support System (DSS) for nuclear emergencies is intended to provide comprehensive and timely information to emergency managers on an emergent situation arising from a nuclear accident. DSS combines the elements of released source term, meteorological conditions, dispersion and deposition in the environment, and estimates the affected areas, exposure of the population and the effects of protective actions on potential dose. The public dose forecast depends, inter-alia, on the accuracy of Numerical Weather Prediction (NWP) data. The National Centre for Medium range Weather Forecast (NCMRWF) provides the NWP forecasts to the Nuclear Power Corporation of India Limited (NPCIL) using a deterministic global model NCUM-G (Rajagopal et al. 2012, Kumar et al.2018, Rani et al.2019). The model forecast has been utilized in various sectorial application such as hydrology (Kumar et al., 2023), renewable energy (Kumar et al., 2022). The surface 10 m wind U and V components forecasted by NCMRWF and transmitted to NPCIL have been compared with observations to evaluate the degree of agreement between the two datasets. The unique aspect of the NCUM-G is that it has a seamless modeling approach. The same dynamical core and, where possible, the same parameterization schemes are used across a broad range of spatial and temporal scales. The UM's dynamical core solves compressible non-hydrostatic equations of motion with semi-Lagrangian advection and semi-implicit time stepping. The NCUM-G model has the Advanced 'ENDGame' (Even Newer Dynamics for General Atmospheric Modelling of the Environment) dynamical core of the Met office, UK. It employs the 'Hybrid 4-D variational data assimilation system, which uses the ensemble forecasts of 'NCMRWF Ensemble Prediction System (NEPS)'. The model has horizontal grid resolution of ~12 km and 70 hybrid vertical levels resolving the atmosphere up to 80km. Full details on the NCUM-G model can be found in Kumar et al (2020). This model is operationally used for generating forecasts out to 10 days based on 00 and 12 UTC initial conditions. The forecasts are used for various applications in diverse sectors ranging from agriculture, renewable energy, early warning for disasters etc. In the inter-comparison study, observed 10m wind speed and direction were compared with the forecasts of wind speed and direction for Indian Nuclear Power Plant (NPP) sites during the period October-2022 to September-2023. NWP data was available with resolution 0.125^{o} x 0.125^{o} for all the Nuclear Power Plant (NPP) Sites. Inter-comparison was conducted for Day-1 to Day-5 forecast lead times. Observed and predicted wind speed and wind direction at 10 m height were used for inter-comparison. To derive wind speed and direction, we utilized the zonal and meridional vectors (U and V) as outlined in the methodology section. The report provides a detailed overview of the NWP winds forecast and an approach of bias correction to make the forecast accurate. The paper has been organized in a way that describes

the NWP model details and datasets used in the study in section 2. Sector 3 highlights the technical details of model evaluation, the statistical metrics used, and the bias correction method. In section 4 we have presented the model evaluation results and discussion of the study over selected NPP locations before and after bias correction. Finally, the results are summarized in section 5.

2. Description of NWP Model and Datasets

2.1 NWP Model Description

NCMRWF Unified model (NCUM) is being used for numerical weather prediction (NWP) since 2012. The NCUM is based on Unified Model (UM) system developed under the "UM Partnership" by Met Office-UK, BoM/CSIRO-Australia, KMA-South Korea, NIWA-New Zealand and MoES/NCMRWF-India. It is a seamless prediction system that runs at all temporal and spatial scales (Kumar et al.2018). A detailed description of early versions and the initial setup of this model has been provided by (Rajagopal et al., 2012, George et al., 2016). This model is upgraded at regular intervals to facilitate new developments in terms of NWP model Physics, data assimilation techniques, and incorporating newly developed datasets in the data assimilation process. The present study is based on the recent model update made in 2018 and 2020 (Niranjan Kumar et al.,2022). The model has a horizontal resolution of ~ 12 km whereas it resolves the atmosphere up to 80 km in 70 vertical levels that include 13 levels within 1 km of the surface to better represent the boundary layer features. The model is initialized at every 6 h (00, 06, 12, and 18 UTC) using the Hybrid 4D-Var data assimilation (Clayton et al.,2013) technique and produces short forecasts at hourly intervals for the next 9 hours. The long forecasts are generated twice a day at 00 and 12 UTC of model runs for up to 240 h in which a few surface parameters such as u and v components of wind speed at 50 m are available at hourly intervals. This fine-resolution NWP model output is useful in wind power forecasting.

2.2 Data Description

NCMRWF model NCUM-G produced forecasts of u and v components of near surface wind speed at 10-m level, 1-hr time intervals from the recent time period October 2022 to September 2023. Model forecasts generated at 00 UTC run up to 120 h forecast length have been evaluated against a high-resolution model analysis. The focus of the study revolves around nine selected Indian

Nuclear Power Plant (NPP) sites Kaiga generating system (KGS), Madras Atomic Power Station (MAPS), Bhabha Atomic Research Centre (BARC), Narora Atomic Power Station (NAPS), Kakrapar Atomic Power Station (KAPP), Kudankulam Nuclear Power Plant (KKNPP), Rajasthan Atomic Power Station (RAPS), Tarapur Atomic Power Station (TAPS), Bhabha Atomic Research Centre Visakhapatnam (BARCV) represented in Figure1.

3. Methodology

3.1Wind speed and Direction Statistics:

(a) Computation of wind speed and direction

The wind speed has been computed from U and V components representing the eastward and northward wind speeds respectively in a Cartesian coordinate system.

$$WS = \sqrt{U^2 + V^2} \quad (1)$$

The wind direction (θ) can then be determined using the arctangent function, given by:

$$\theta = atan2(U,V) \quad (2)$$

(b) Estimation of Wind Direction Difference:

Wind direction difference θ = predicted wind direction – measured wind direction If $\theta > 180^o$, then wind direction difference $\theta=\theta-360^o$ If $\theta < -180^o$, then wind direction difference $\theta=\theta+360^o$

(c) Calculation of Average Wind Direction: From the sequence of N observations θi and ui, the mean east-west, Ve and north-south, Vn, components of the wind are:

$$Ve= - 1/ N \sum Uisi(\theta i) \text{ and } Vn=- 1 /N \sum Uicos(\theta i) \quad (3)$$

Geographic wind direction with respect to true north (0=North, 90=East, 180=South, 270=West) that the wind is coming from is given by

$$Dir_{geo} =270-(atan2(Vn, Ve)) \quad (4)$$

Average wind direction as discussed in this section is used for calculating hourly averaged wind direction for the period of inter-comparison.

(d) Calculation of Mean Absolute Error (MAE) in wind direction:

Wind direction difference is calculated as per the methodology given in Section (a).

MAE in wind direction is estimated as per below equation:

$$\text{MAE (direction)} = 1/N \sum \min(|\delta Oi - \delta Fi|, |360° + \delta Oi - \delta Fi|, |360° + \delta Fi - \delta Oi|)N \quad (5)$$

Where δOi and δFi are observed and forecast wind directions respectively.

3.3 Statistical measures for inter-comparison of observed and predicted

Statistical metrics such as BIAS, MAE (mean absolute error), RMSE (root mean square error), CC (correlation coefficient) have been computed using the equations/formulae as follows:

$$\text{MAE} = \frac{1}{n}\sum_{i=1}^{n}|Observed_i - Forecast_i| \quad (6)$$

$$\text{RMSE} = \sqrt{\frac{1}{n}\sum_{i=1}^{n}(Observed_i - Forecast_i)^2} \quad (7)$$

$$\text{CC} = \frac{\sum_{i=1}^{n}\left(Observed_i - \overline{Observed}\right)\left(Forecast_i - \overline{Forecast}\right)}{\sqrt{\sum_{i=1}^{n}\left(Observed_i - \overline{Observed}\right)^2 \sum_{i=1}^{n}\left(Forecast_i - \overline{Forecast}\right)^2}} \quad (8)$$

$$\text{MBE} = 1/n\sum_{i=1}^{i=n}(Forecast - observed) \quad (9)$$

Where, n is the length of the datasets being compared, Forecast and Observed values correspond to NSPS model forecast and analysis respectively, whereas Forecast and Observed represent the mean values of it.

3.3 Bias correction

NWP model forecasts face inherent challenges stemming from imperfect initial conditions, numerical approximations, and the simplification of numerous atmospheric processes, all contributing to specific biases (Cheng and Steenburgh, 2005; Coleman et al., 2010; Kalman R.E., 1960) which are more prominent for surface and boundary-layer parameters such as winds (Cheng et al., 2013). This study aims to rectify the bias in the forecasts of wind speed from the NCUM- G

model for the period October 2023 to September 2023. This correction process involves the application of a technique outlined below:

Moving Average Bias Correction (MABC): The technique adopted in this is simple and easy to implement in an operational environment. Its uses have been well demonstrated by (Cui et al., 2012; Singh et al., 2020). This approach involves estimating the bias (difference between forecast and observation) as a weighted average of biases from the three most recent hours of available data. Bias correction is conducted separately for each hour in the next 6- hour forecast dataset. The bias has been calculated using Eq. 10.

Bias (t) = 0.4 * b1+ 0.4 * b2 + 0.2 * b3 (10)

Where b1, b2, and b3 are the biases in the last 3 hours of forecasts.

After estimating the bias, the wind speed forecast undergoes correction by subtracting this estimated bias using the Eq. 9.

$Fb(t)$=F (t) - Bias (t) (11)

Where 't' is the forecast hour, $Fbc(t)$ denotes the bias corrected forecast, F(t) represents NCUM-G raw forecast and Bias(t) signifies the bias calculated in equation (11).

4. Results and discussions

4.1 NWP Model Evaluation

The focus of the study revolves around nine selected Indian Nuclear Power Plant (NPP) sites represented in Figure1. The model orography has also been presented in Figure1 . From the figure, we can infer that the NPP in Gujarat, Rajasthan and Delhi are located at relatively lower elevation whereas wind farms in Maharashtra and Karnataka are located at the highest elevation. The local topography affects the weather phenomenon which at many instances may not be well represented by the NWP models due to their coarser resolution.

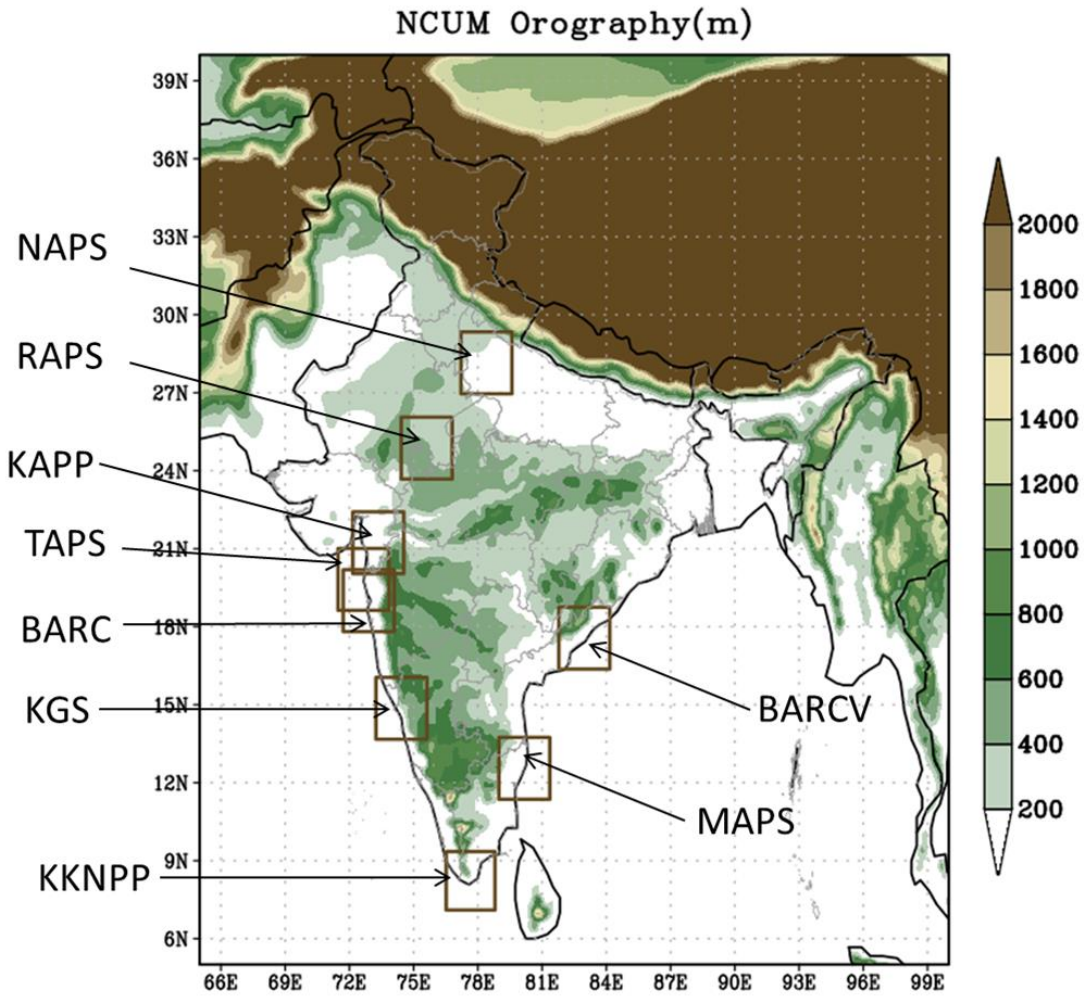

Figure1: Model orography that highlights the terrain at selected Nuclear Power plant (NPP) sites.

The NWP model output provides U and V components of winds at 10 m above ground level that have been used to compute the speed and direction. The annual mean of WS and WD together have been represented in Figure 2. From the plots we can compare the forecast and analysis of these parameters at different lead times. The length of vectors and shading in the plot represents the wind speed whereas the orientation tells us about the direction. The plots facilitated a qualitative assessment of the spatial distribution of the forecasted wind vectors in comparison to the model analysis. We can infer the following features from the figure: (a) strong south-westerlies over the Arabian Sea (AS) with core winds exceeding 7 m/s, (b) south-westerlies over Bay of Bengal (BoB), (c) westerlies over peninsular and central India. The mean wind speeds consistently surpass the threshold of 4 m/s across all sites whereas specific regions within Rajasthan and

Gujarat exhibit even more elevated wind speeds, exceeding 5 m/s. The figure shows that the spatial pattern of wind speed forecast is well captured in day -1,3 and 5 lead times. However, a discrepancy is seen in certain regions, notably over the seas in day 3 and day 5, where a tendency for overestimation that increases with lead times was evident.

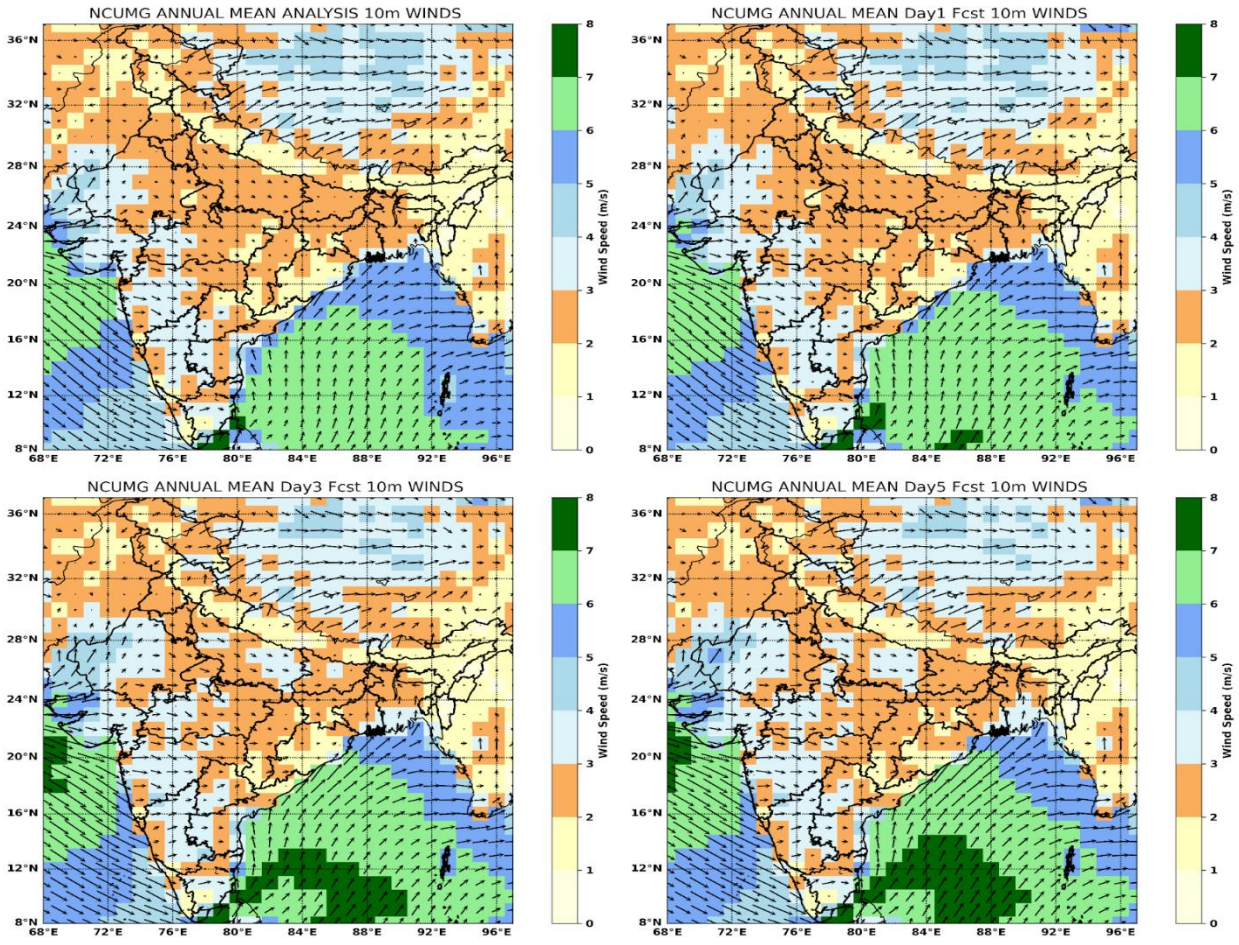

Figure 2: Wind Vector Plot comparing model analysis wind vectors to forecast wind vectors for Day 1, Day 3, and Day 5 ahead, on an annual basis for the period October 2022 to September 2023.

Figure 3 presents the Root Mean Square Error (RMSE) for Day 1, Day 3, and Day 5 lead time WS forecasts compared to the model analysis, spanning from October 2022 to September 2023. In the Day 1 forecast, the RMSE across most of India remains below 1 m/s, indicating generally accurate predictions. However, certain regions in the western part of Rajasthan exhibit slightly higher RMSE values, ranging up to 1.2 m/s, suggesting a moderate discrepancy between forecasted and

observed WS. For the Day 3 forecast, the RMSE is predominantly below 1.2 m/s across most parts of India, indicating relatively accurate forecasts. However, in northern India, particularly in the western part of Rajasthan and some areas in northern Gujarat, the RMSE exceeds 1.2 m/s, with values up to 1.6 m/s. This suggests a slightly larger deviation between forecasted and observed WS in these regions. In the Day 5 forecast, the RMSE remains below 1.4 m/s across the majority of India, indicating higher deviation compared to the Day 1 and Day 3 forecasts . Nonetheless, in the western part of Rajasthan and certain areas in northern Gujarat, the RMSE is below 1.8 m/s, with some regions in Rajasthan showing RMSE values exceeding 2 m/s. This indicates a notable deviation between forecasted and observed wind speeds, particularly in these specific areas. The results suggest that model forecast accuracy in the first 24 hours (Day1) is reasonably good and decreases appreciably at higher lead times.

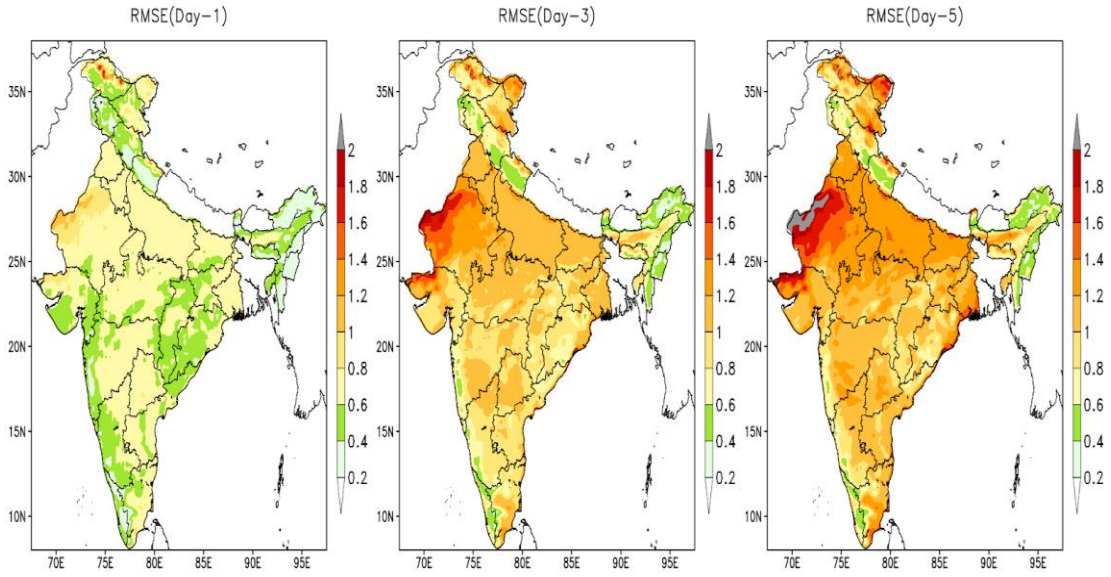

Figure 3: Root Mean Square Error (RMSE) in Day 1, Day 3, and Day 5 ahead forecasts in comparison to model analysis, spanning the period from October 2022 to September 2023.

To examine any seasonal dependency in WS, Figure4 shows the mean annual cycle of the analysis and forecast WS averaged over each of the nine NPCIL sites from October 2022 to September 2023, for Day 1, 3, and 5 lead times. At certain sites, such as KGS, KKNPP the match at all lead times is notably good, suggesting better agreement between forecasted and observed wind speeds. The reasons for this enhanced performance at these specific sites could be attributed to various factors such as geographical location, and the local topography. The figure provides a

comprehensive overview of mean WS across seasons and years, allowing for a clear comparison between the sites and revealing significant seasonal patterns. The data reveals notable seasonal patterns, with the highest mean WS observed during the summer months May to September, which can be characterized as the high wind season. The findings from the analysis indicate that the Day 1 forecast closely aligns with the model analysis, suggesting a high level of accuracy in short-term WS predictions. However, biases in WS forecasts become more pronounced with increasing lead times. Further, the study reveals that these biases are particularly prominent during the summer months from May to September.

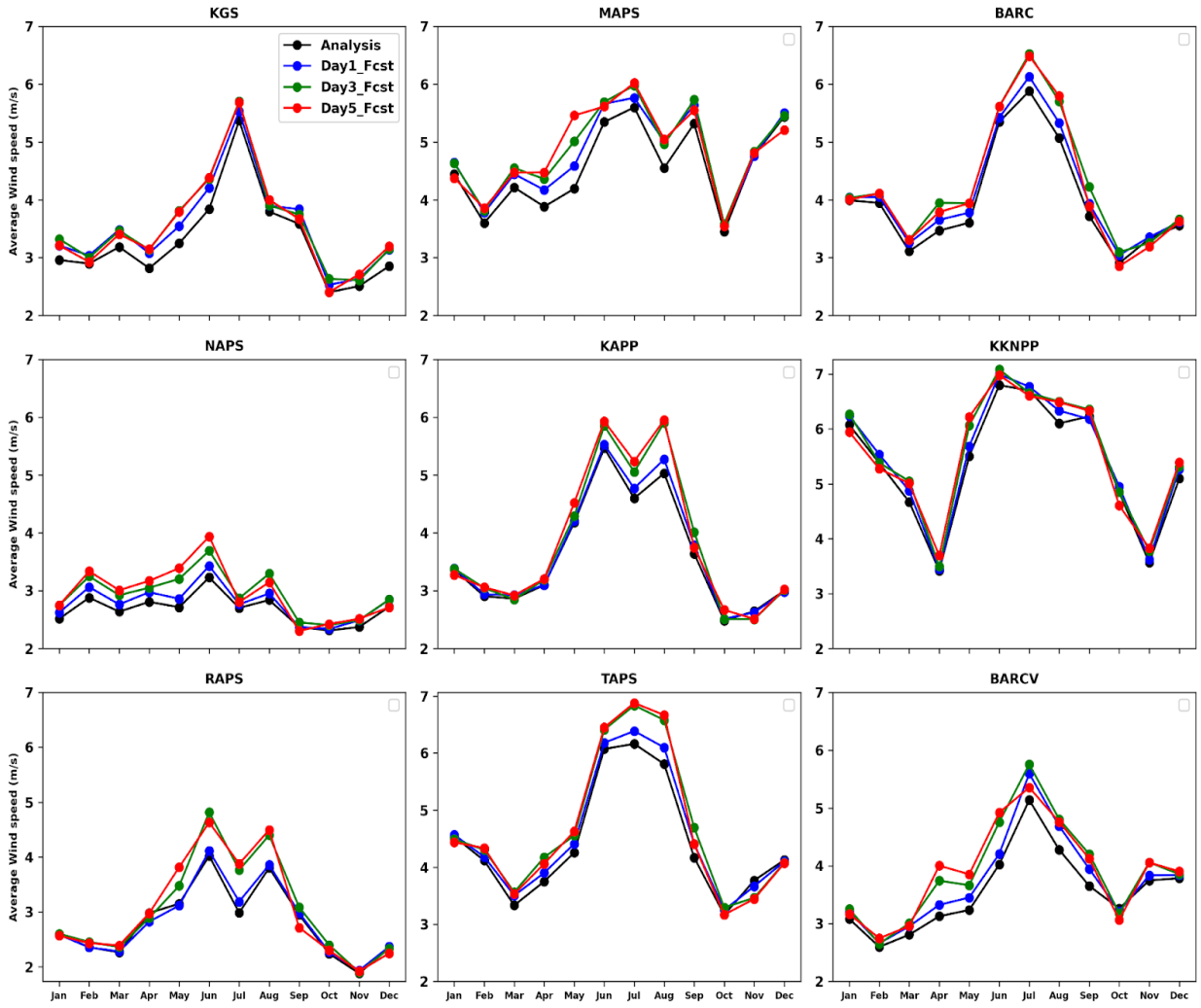

Figure4: Mean annual cycle of the observed and forecast wind speed averaged over each of the nine NPCIL sites during October 2022 - September 2023 for lead time Day1, Day3 and Day5.

The mean annual cycle of analysed and forecast WD was examined across nine NPCIL sites from October 2022 to September 2023, considering lead times of Day 1, Day 3, and Day 5. The analysis aimed to identify any seasonal dependency in wind direction and assess the accuracy of wind direction predictions. The results, presented in a comprehensive Figure5, allowed for a clear comparison between sites and revealed significant seasonal patterns. Notably, the data indicated that the dominant wind direction during the summer months from May to September is south westerly direction. The findings suggest that the five-day ahead forecast closely aligns with the model analysis, indicating a high level of accuracy in WD prediction even at higher lead times. However, slight biases in wind direction forecasts are observed for certain sites during specific months. For example, the NAPS site exhibited small biases in wind direction forecasts during the summer months from May to September, while the BARCV site showed similar biases during the months of March to May. Despite these minor deviations, the overall accuracy of the forecasted wind direction remained high across all lead times.

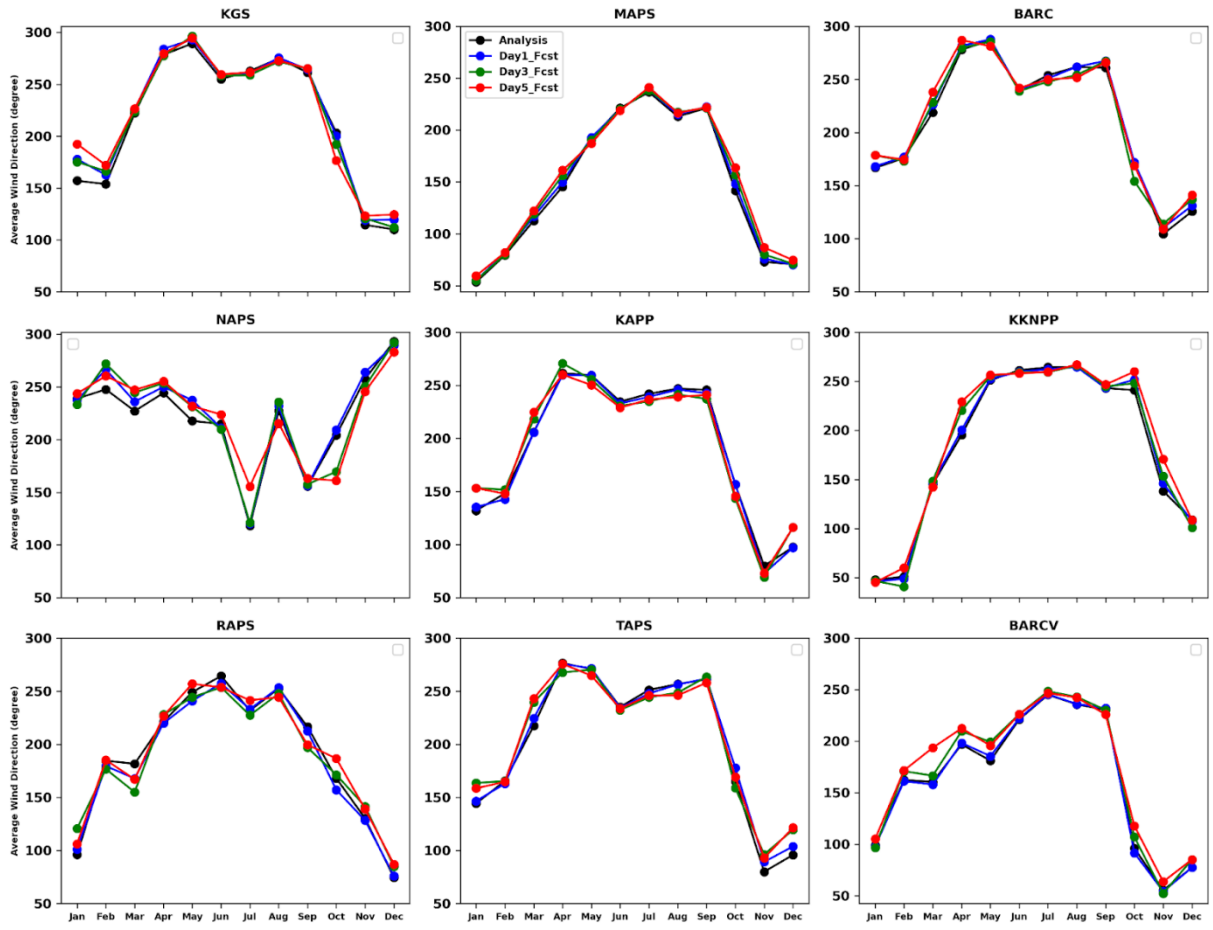

Figure 5: Mean annual cycle of the analysed and forecast wind direction averaged over each of the nine NPCIL sites during October 2022 - September 2023 for lead time Day1, Day3 and Day5.

The mean diurnal variation of hourly wind speeds across the nine selected NPP sites have been presented in Figure 6. The data reveals a compelling pattern in the fluctuations of wind speed throughout a typical day. The findings indicate that the wind speeds exhibit a consistent rhythm with lower values during the early morning and a gradual increase through the day, peaking in the late afternoon. Notably, the MAPS site exhibits consistent wind speeds throughout the day, distinguishing it from the observed pattern. Additionally, sites such as KKNPP, MAPS, and TAPS display elevated wind speeds during the morning hours as well, with KKNPP recording the highest mean wind speed during this time. Furthermore, the analysis highlights significant differences in the range between maximum and minimum wind speeds over a 24-hour period, particularly notable in sites KGS, BARC, and KAPP. These findings provide valuable insights into the

temporal dynamics of wind speed across NPP sites, crucial for understanding and refining their operational approaches.

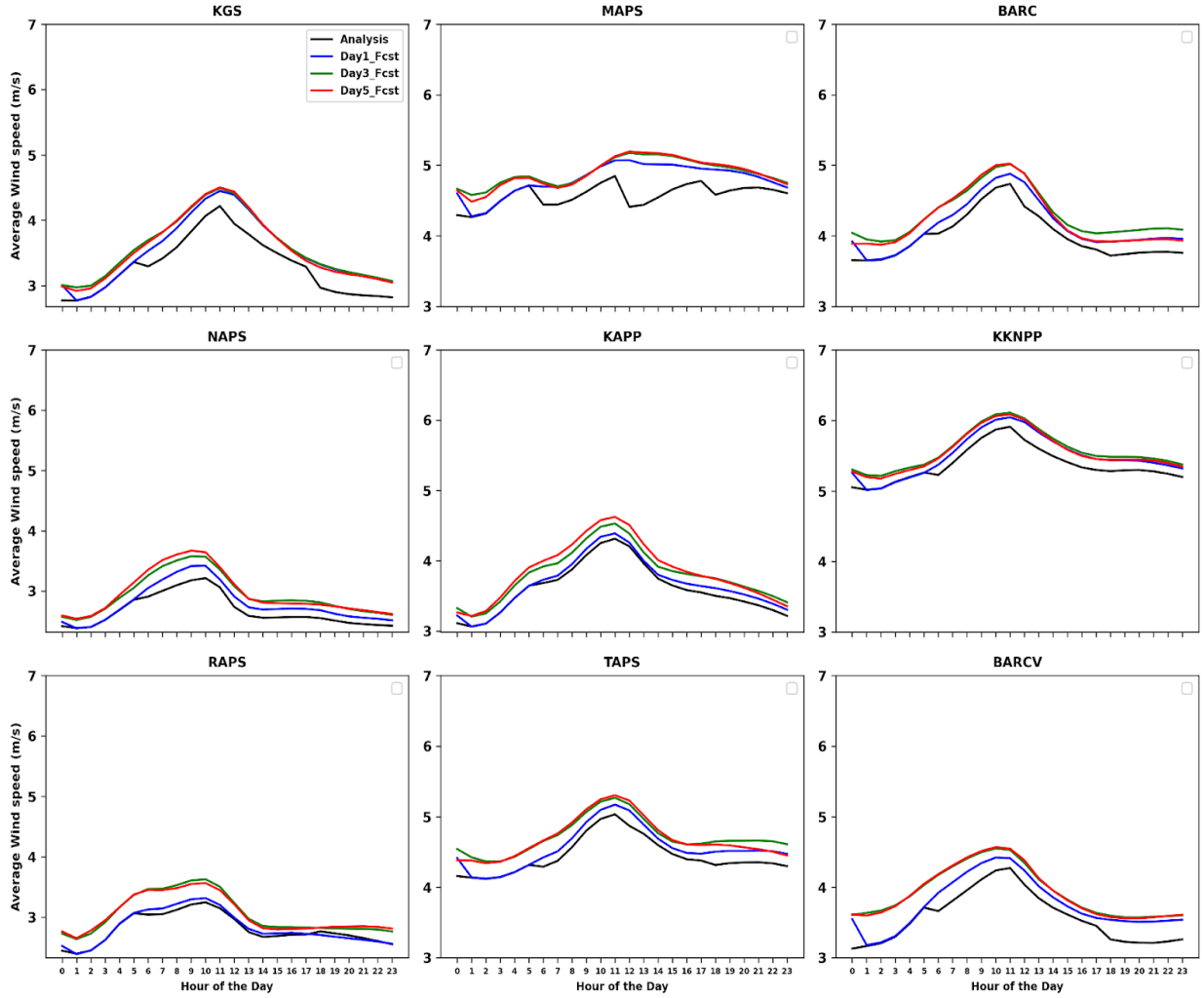

Figure 6: Mean diurnal cycle of the analysed and forecast wind speed averaged over each of the nine NPCIL sites during October 2022 – September 2023 for lead time Day1, 3 and 5.

The WD provides a crucial input to the DSS making it an important parameter to be critically analysed. It helps us identify the regions to be evacuated during any nuclear emergency. In Figure 7, the mean diurnal variation of hourly wind direction across the nine selected NPP sites has been presented. From the figure we infer that the diurnal variability in the wind direction is different at different NPP sites. Two NPP sites KKNPP and BARCV show a little variability and these sites are dominant by the southerly winds whereas KGS, BARC, and TAPS show relatively higher

variability. These three sites witness north- westerly winds in the evening. From the assessment of model forecasts provided in the figure we broadly observe that the diurnal variability of forecasts even at higher lead times are in a good agreement with the model analysis over all the sites.

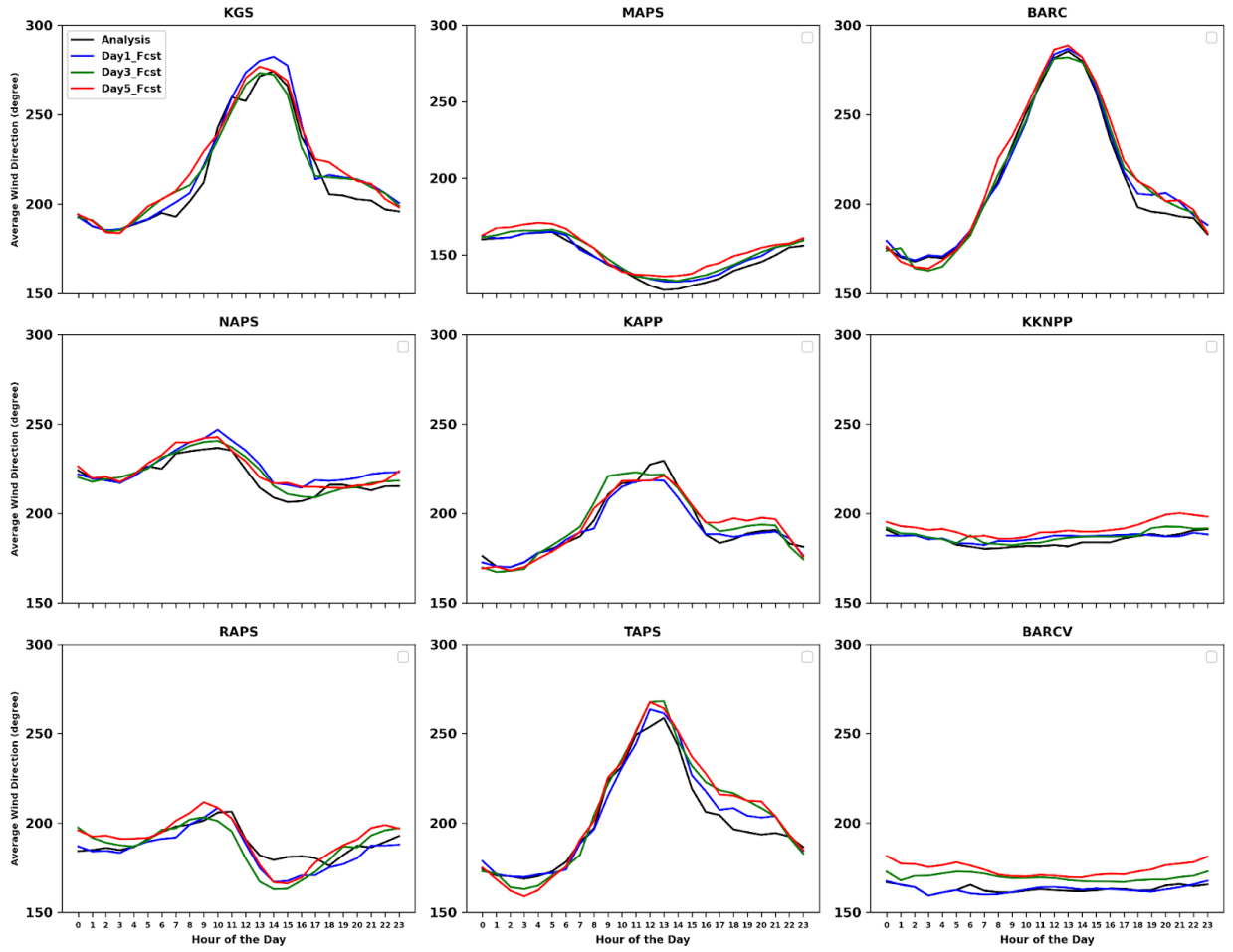

Figure 7: Mean diurnal cycle of the analysis and forecast wind direction averaged over each of the nine NPCIL sites during October2022 - September2023 for lead time Day1,3 and 5.

The scatter plots depicting the association between analysis and forecasted (Day-1) wind speeds across the nine NPCIL sites from October2022 to September 2023, as shown in Figure 8, reveal a notably strong relationship. Each plot showcases a high level of association, as evidenced by the R^2 values exceeding 0.88 for all sites. This indicates a robust correlation between the analysed and forecasted wind speeds, affirming the accuracy and reliability of the forecasting model utilized. These findings underscore the effectiveness of the forecasting approach in accurately predicting

wind speeds at each NPCIL sites, which is essential for informed decision-making and operational planning.

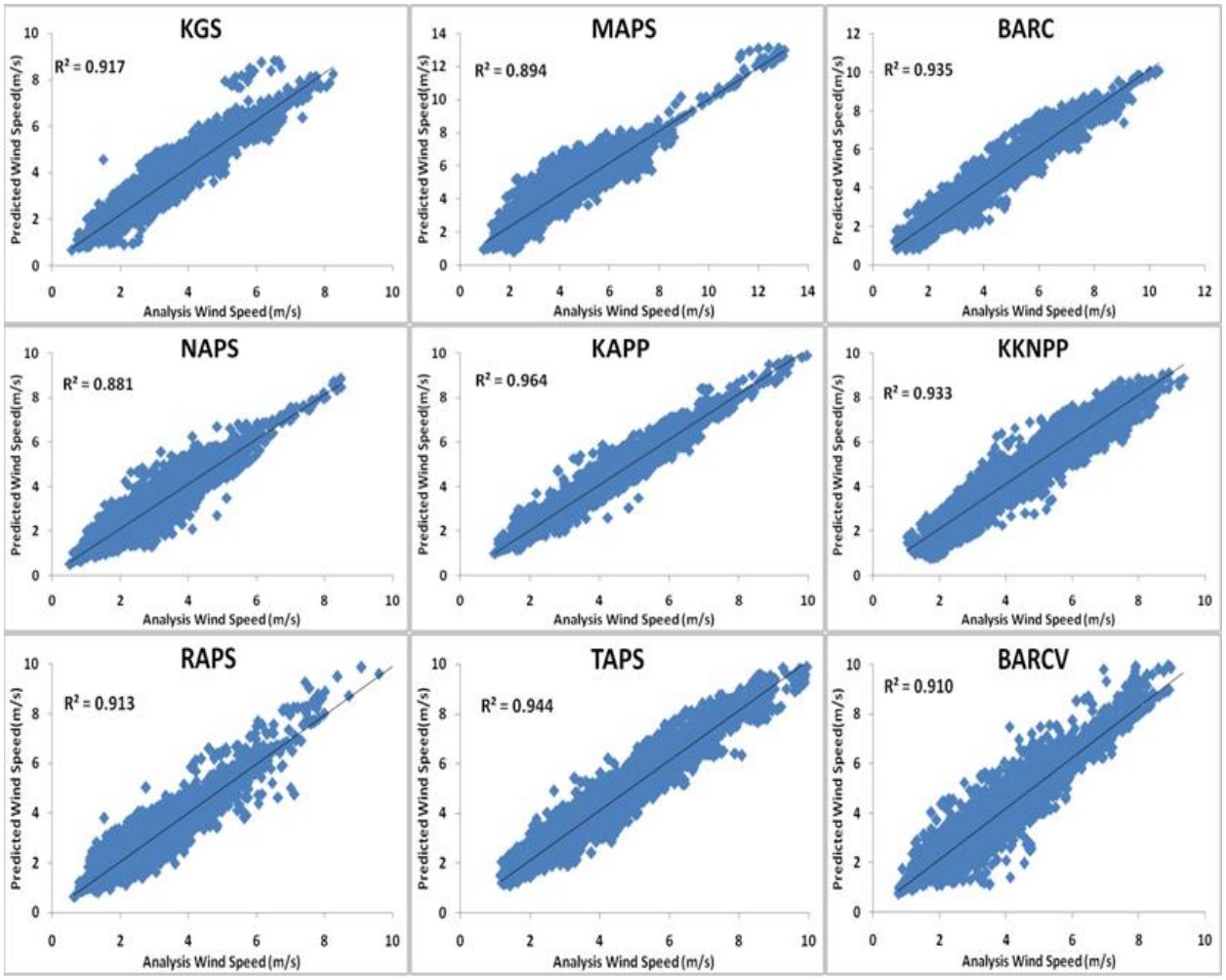

Figure 8: Scatter plot of observed Vs forecast hourly wind speed (m/s) averaged over each of the nine NPCIL sites from October 2022 to September 2023. The plots indicate very good association as indicated by R^2 values in each panel.

The scatter plots depicting the association between analysis and forecasted (Day 1) wind direction across the nine NPP sites, as shown in Figure 9, reveal a notably strong relationship. Each plot showcases a moderate association, as evidenced by the R^2 values exceeding 0.77 for all sites except for the sites NAPS (.68), RAPS (.69) and TAPS (.73) where R^2 values are less as compared to other sites.

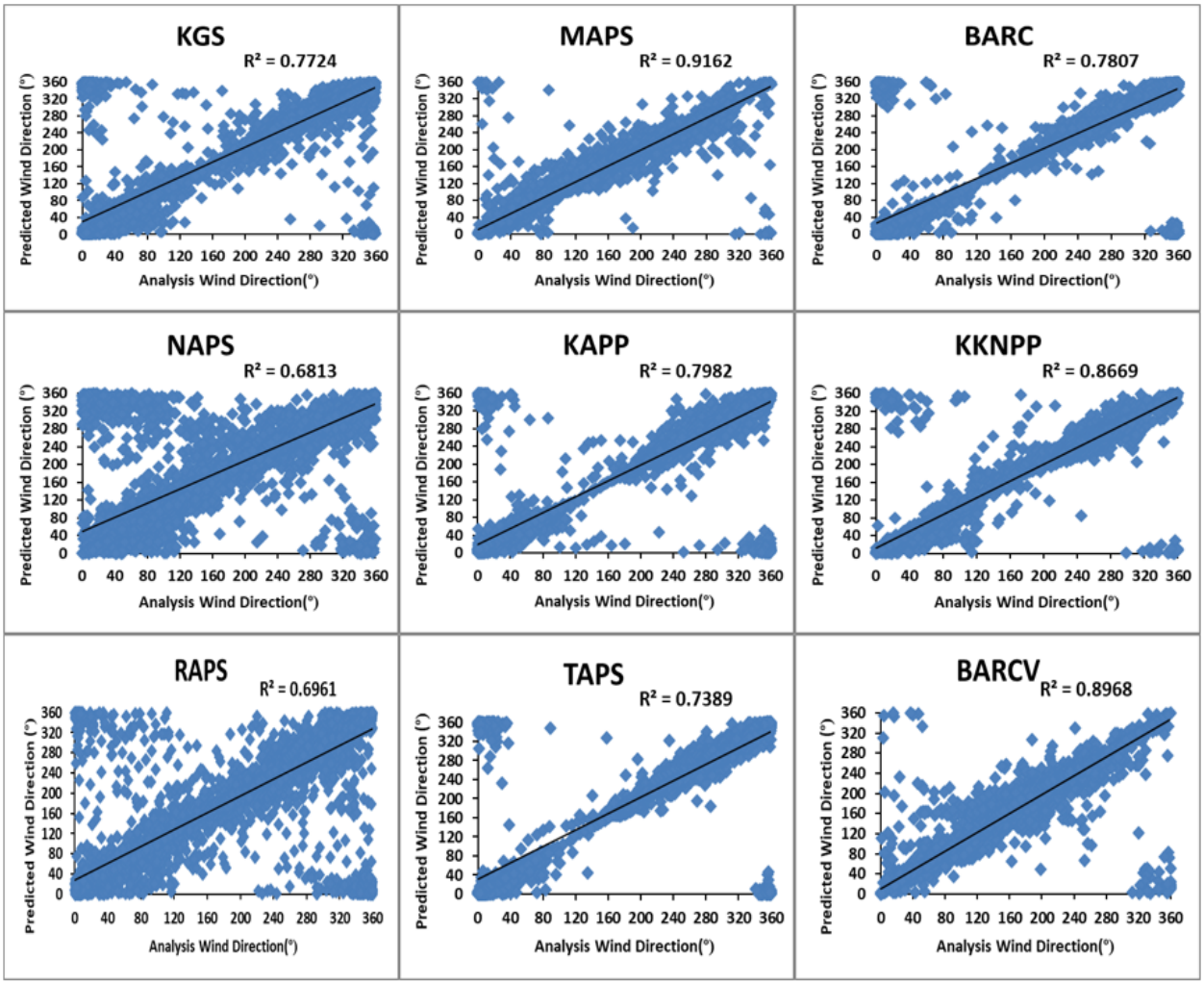

Figure 9: Scatter plot of observed Vs forecast hourly wind direction (degree) averaged over each of the nine NPCIL sites from October 2022 to September 2023. The plots indicate moderate association as indicated by R^2values in each panel.

The distribution of WS across different categories was analyzed to evaluate forecast accuracy and identify potential biases or errors in the Day-1 forecast as shown in Figure 10. The wind speed categories ranged from less than 2 m/s, 2-4 m/s, 4-6 m/s, 6-8 m/s, to greater than 8 m/s. The analysis, depicted in Figure 10, revealed that the highest proportion, over 60%, fell within the WS range of 2-4 m/s, except for KKNPP at 20%, MAPS at 30%, and TAPS at 40%. Notably, KKNPP exhibited a distribution of high wind speeds (6-8 m/s) exceeding 40%. Conversely, less than 10% of the data corresponded to wind speeds below 2 m/s across most sites, except for NAPS and RAPS

where it was around 30%. Furthermore, these two sites showed negligible wind speeds above 6 m/s. KKNPP stood out again with 40% of its data falling within the 6-8 m/s WS range. Importantly, the results concludes that the forecast distribution for each WS range closely matched the model analysis, indicating reliability in the forecasting approach.

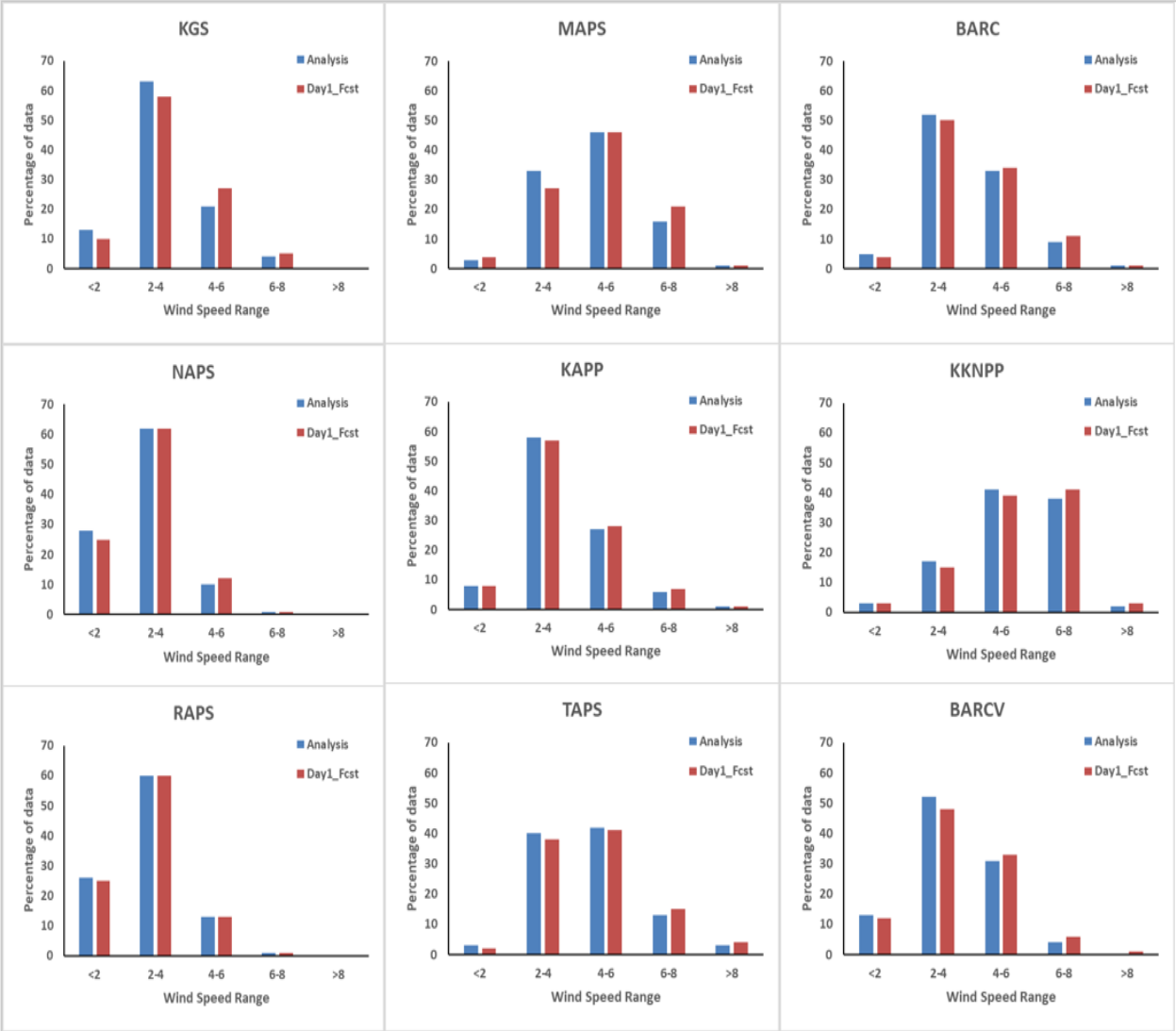

Figure 10: Frequency distribution (%) of Analysis and Forecast (Day-1) wind speed averaged over each of the nine NPCIL sites, spanning the period from October 2022 to September 2023.

The box plot in Figure 11 provides a comprehensive visualization of the spread of Analysis and Day-1 Forecast wind speed averaged over nine NPCIL sites, during the study period[A1]. The box

itself represents the interquartile range (IQR), encapsulating the middle 50% of the data points, with the horizontal line inside indicating the median WS. Whiskers extend to the maximum and minimum values within 1.5 times the IQR from the upper and lower quartiles, serving as a measure of data variability. Notably, the figure reveals a close alignment between the average WS of Day-1 forecast and the model analysis, underscoring the reliability of the forecasting model. However, slight differences in the IQR for each month suggest a small tendency for overprediction. Furthermore, discernible seasonal patterns emerge, with the highest mean WS occurring during the summer months from May to September, indicative of a distinct high wind season. This detailed analysis of wind speed distribution provides valuable insights into the performance of the forecasting model and highlights the influence of seasonal variability on wind patterns.

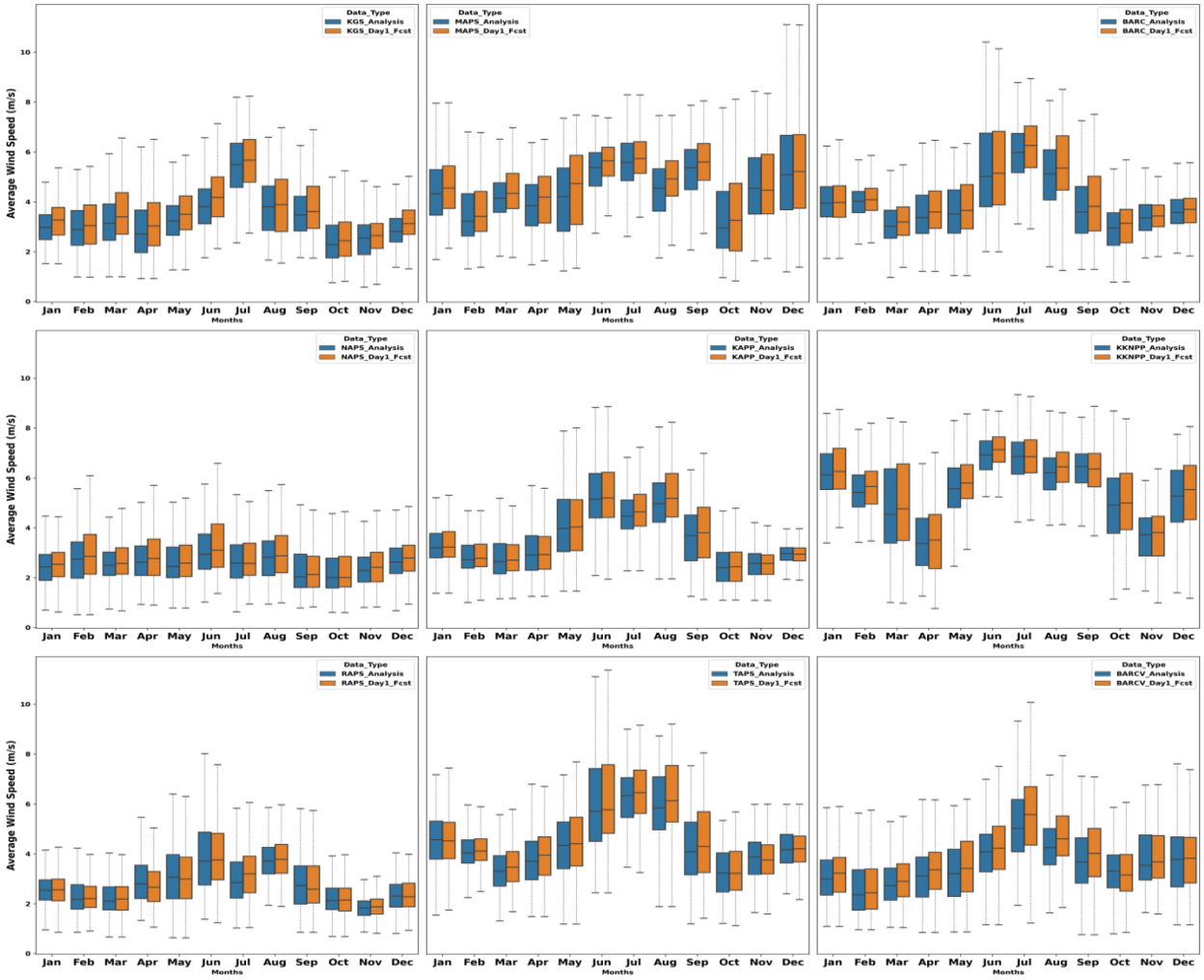

Figure 11: Box plot illustrating the Analysis and Forecast (Day-1) wind speed averaged over nine NPCIL sites from October 2022 to September 2023. The box represents the interquartile range (IQR), with the median indicated by the horizontal line inside the box. Whiskers extend to the maximum and minimum values within 1.5 times the IQR from the upper and lower quartiles, respectively.

This study also delves into the examination of the Mean Absolute Error (MAE), as depicted in Figure 12, in Day 1 wind speed forecasts compared to model analysis within a designated latitude-longitude range across nine sites. This investigation spanned the timeframe from October 2022 to September 2023, aiming to assess the accuracy of the forecasting model in predicting wind speed to these sites. The results contribute to a comprehensive understanding of the model's performance and its implications for forecasting accuracy in the context of NPP site monitoring and analysis.

The results revealed consistently low MAE values across all nine sites, with each site exhibiting MAE values below 1 m/s. Particularly, the sites KAPP, TAPS, NAPS, and RAPS, where the MAE consistently remained below 0.6 m/s across all grids. However, slight variability was observed among the other sites, with some grids registering MAE values above 0.7 m/s. Notably, certain grids within the KGS site exhibited higher MAE values exceeding 0.8 m/s. These findings highlight the overall reliability of the forecasting model, albeit with minor deviations observed in specific grid areas and sites.

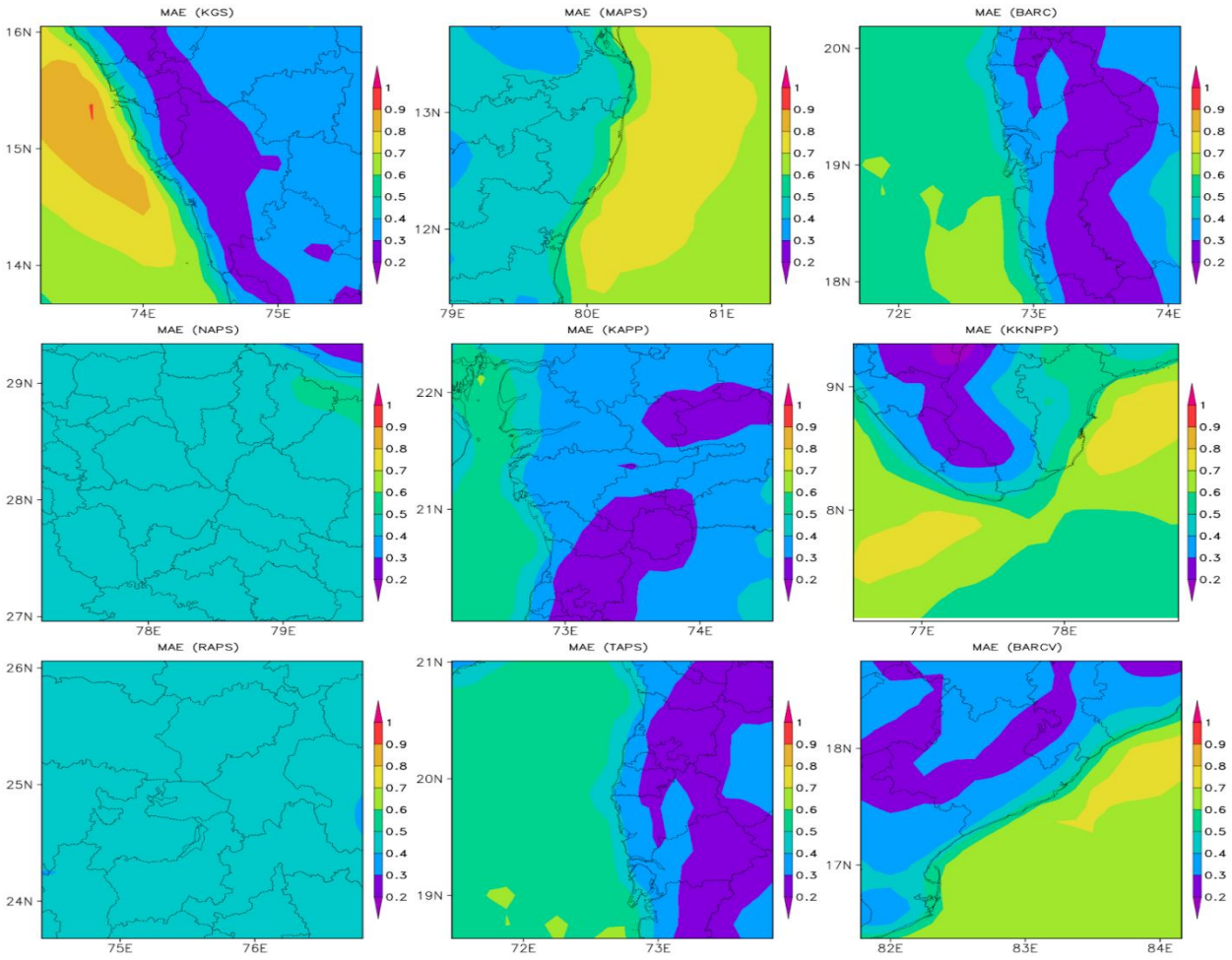

Figure12: MAE in Day 1 forecasts in comparison to model analysis at each grid within a latitude-longitude box for 9 NPP sites, spanning the period from October 2022 to September 2023.

The model performance for wind speed forecast has also been examined in terms of RMSE , as depicted in Figure 13. The Day 1 forecast is compared to model analysis within a designated latitude-longitude range across nine NPP sites from October 2022 to September 2023. The results

revealed consistently low RMSE values across all nine sites, with each site exhibiting RMSE values below 1.3 m/s. Particularly, the sites KAPP, TAPS, NAPS, and RAPS, where the RMSE consistently remained below 0.9 m/s across all grids. However, slight variability was observed among the other sites, with some grids registering RMSE values above 1.1 m/s. Notably, certain grids within the KGS site exhibited higher RMSE values exceeding 1.3 m/s. These findings underscore the overall reliability of the forecasting model, albeit with minor deviations observed in specific grid areas and sites.

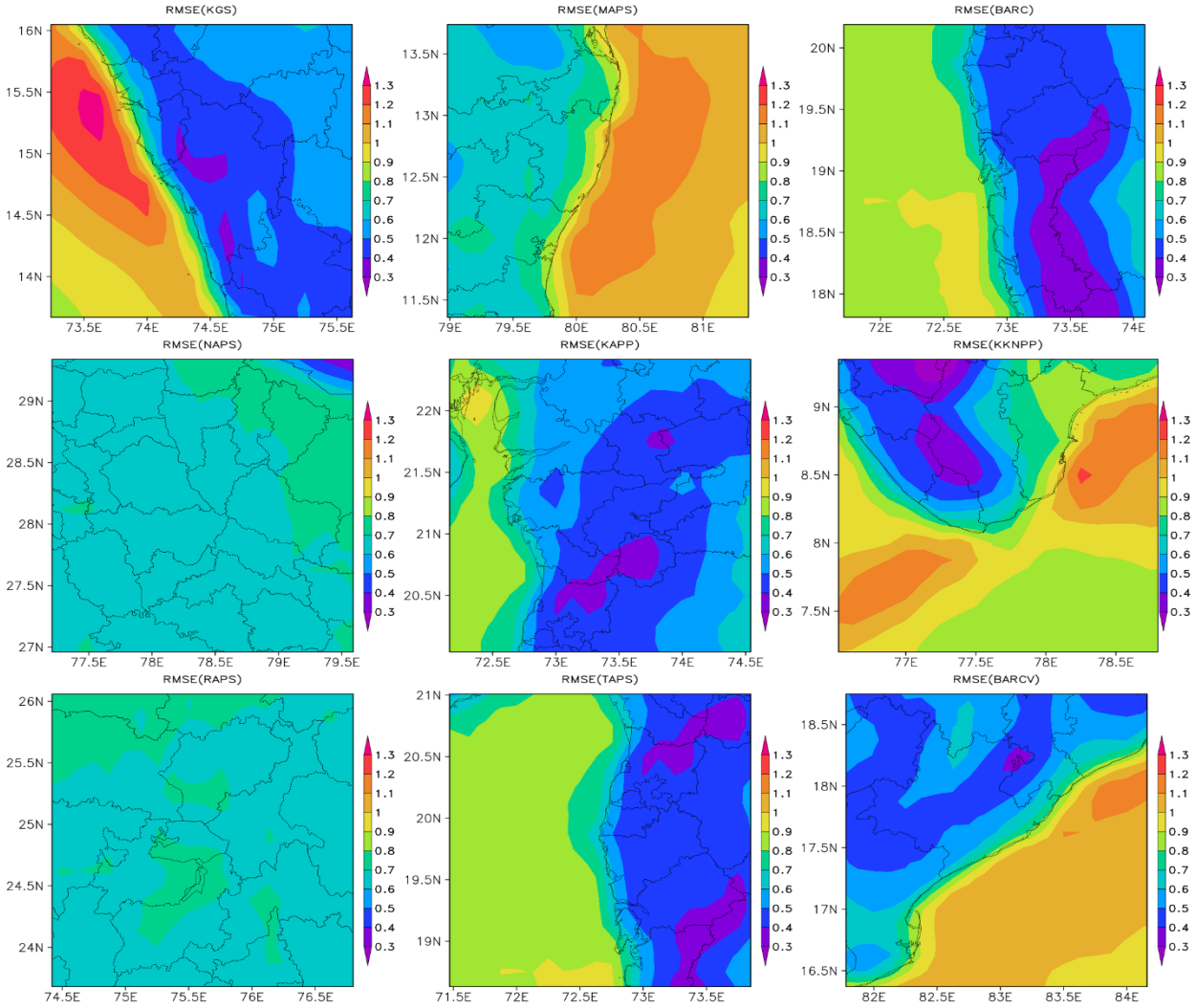

Figure 13: RMSE in Day 1 forecasts in comparison to model analysis at each grid within a latitude-longitude box for 9 NPP sites, spanning the period from October 2022 to September 2023.

The study examined seasonal variations in wind speed forecasts averaged over nine NPP sites during the study period, considering lead times of Day-1, 3, and 5. Figure 14 illustrates the MAE in forecasted WS compared to the analysis. Notable seasonal patterns emerged, with the highest MAE occurring during the summer months (May to September), known as the high wind season. Differences in MAE throughout the months were more pronounced for Day-3 and Day-5 forecasts compared to Day-1. The Day-1 forecasts showed minimal variation in MAE across the months, particularly at the KKNP site where MAE remained nearly constant. Additionally, the MAE for Day-1 forecasts was consistently below 0.5 m/s across all sites, while Day-3 and Day-5 forecasts exhibited higher MAE values. Specifically, Day-3 forecasts had an MAE below 1 m/s for all sites, while Day-5 forecasts reached up to 1.5 m/s for certain sites. The results conclude that biases in wind speed forecasts became more pronounced with increasing lead times. These findings provide valuable insights into understanding seasonal variations and the impact of lead times on wind speed forecast accuracy, crucial for various applications including energy production and infrastructure planning.

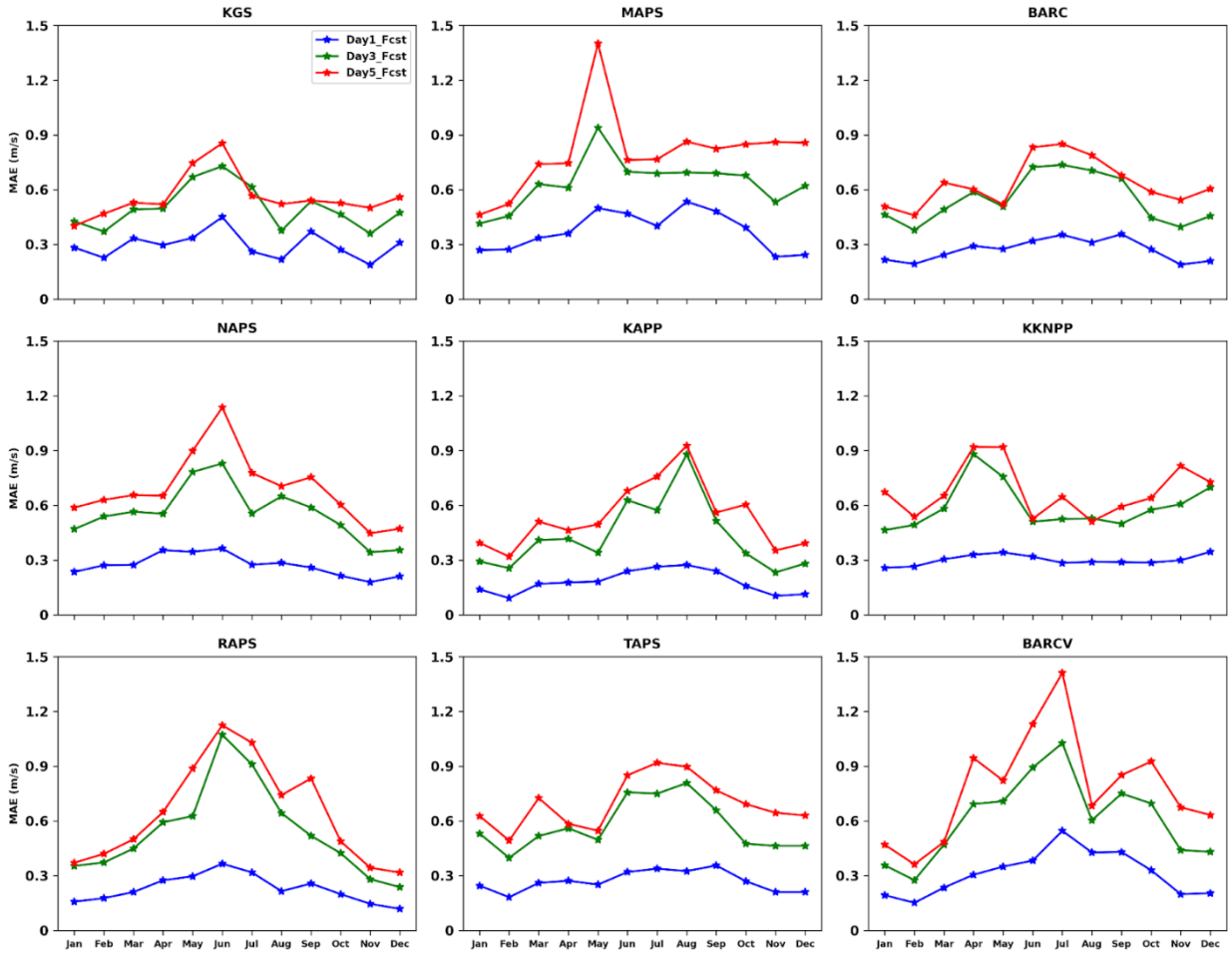

Figure 14: Annual variation in the Mean Absolute Error (MAE) in forecast wind speed (against analysis) averaged over latitude-longitude for each of the nine NPP sites for lead times Day-1, 3 and 5.

The study examined seasonal variations in wind direction forecasts across nine NPCIL sites during the study period, for Day-1, 3 and 5 lead times. Figure 15 illustrates the MAE in forecasted wind speeds compared to analysis. Notable seasonal patterns emerged, with the highest MAE occurring during the winter months (Jan to April, October to September), known as low wind season. Differences in MAE throughout the months were more pronounced for Day-3 and 5 forecasts compared to Day-1. The MAE for Day-1 forecasts was consistently below 25 degrees across all sites except for KGS in winter season it reaches to 40 degrees , while Day-3 and Day-5 forecasts exhibited higher MAE values. Specifically, Day-3 forecasts had an MAE below 70 degrees for all sites and for Day-5 forecast MAE reached up to 95 degrees for RAPS sites. The results conclude

that biases in wind direction forecasts became more pronounced with increasing lead times. These findings provide valuable insights into understanding seasonal variations and the impact of lead times on wind speed forecast accuracy, crucial for various applications including energy production and infrastructure planning.

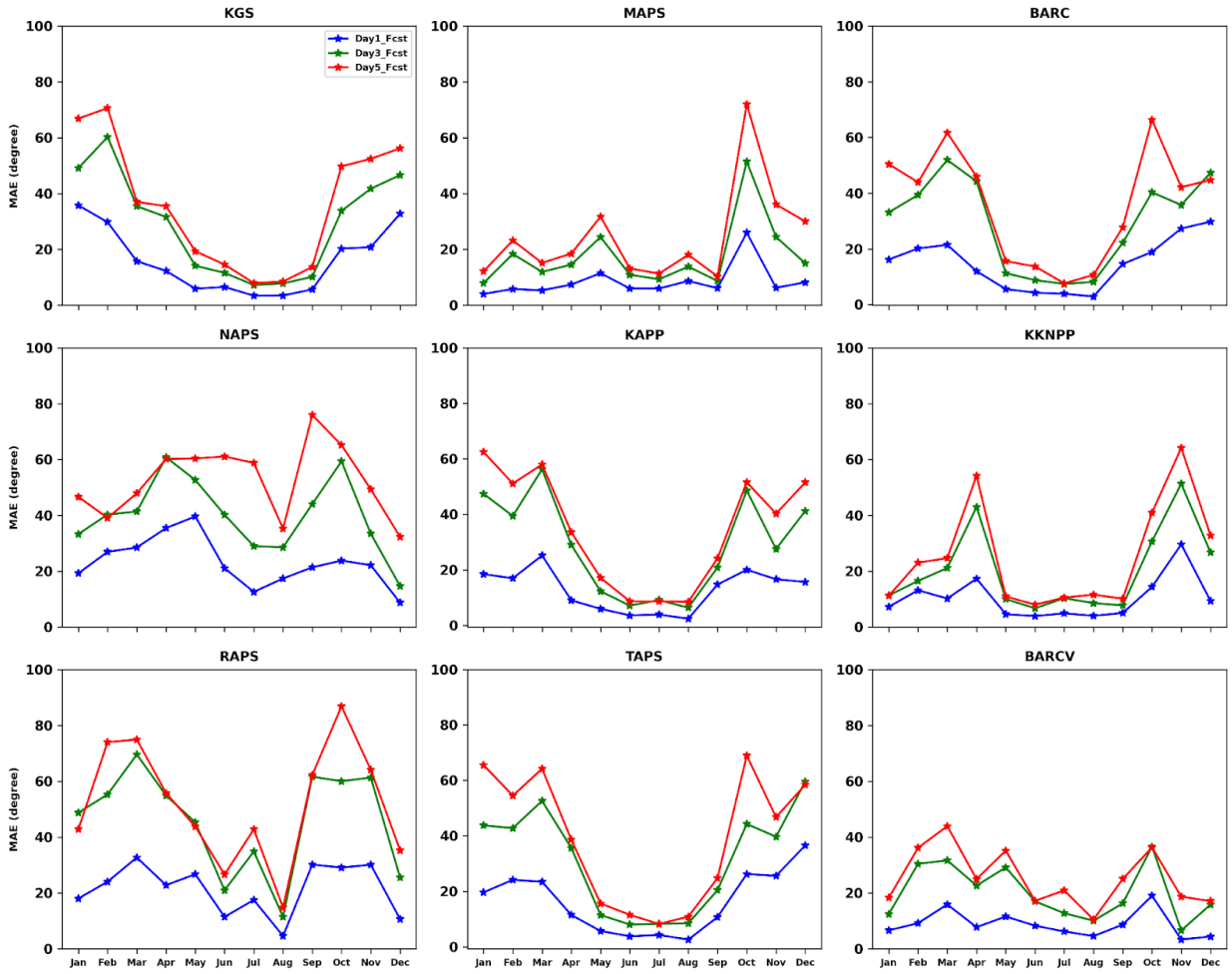

Figure 15: Annual variation in the MAE in forecast wind direction (against analysis) averaged over latitude-longitude for each of the nine NPCIL sites during October 2022-Sep 2023 for lead times Day-1, 3 and 5.

The diurnal variation of MAE in hourly wind speeds across nine selected NPP sites has been examined, as depicted in Figure 16. The results uncovers a notable pattern in wind speed fluctuations over a typical day, revealing a consistent rhythm characterized by lower MAE values during the early morning and a gradual increase throughout the day, reaching a peak in the late

afternoon. Particularly, on Day 1 of the forecast, MAE remains below 0.5 m/s for all NPP sites except for MAPS where it reaches to 1 m/s. Specifically, Day-3 forecasts had an MAE below .9 m/s for all sites, while Day-5 forecasts reached up to 1.2 m/s for certain sites. Moreover, the results highlight that MAE tends to escalate with higher lead time. These findings offer valuable insights into the temporal dynamics of wind speed across NPP sites

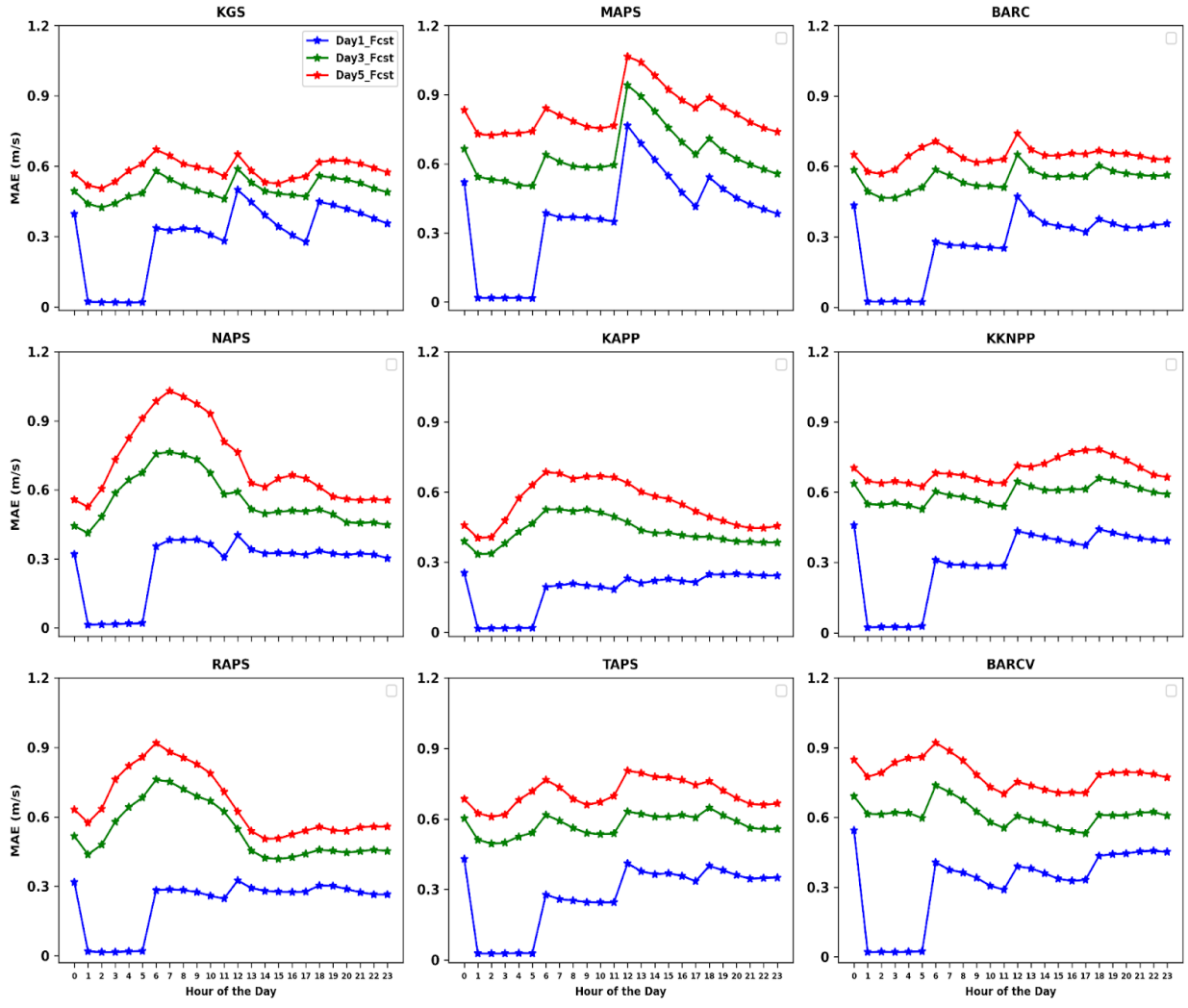

Figure 16: Diurnal variation in the MAE in forecast WS (against analysis) averaged over latitude-longitude for each of the nine NPCIL sites during October 2022-September 2023 for lead times Day-1, 3 and 5.

The diurnal variation of MAE in hourly WD across nine NPP sites has been investigated, revealing a consistent pattern in WD fluctuations over a typical day. The results show that MAE values are generally lower during the early morning and gradually increase throughout the day. Specifically, in the Day1 forecast, MAE remains below 20 degrees for most NPP sites, except for KGS, NAPS, and RAPS, where it reaches 40 degrees. In Day3 forecast, MAE is generally below 40 degrees, but exceeds this threshold for NAPS, RAPS, and BARCV. In Day 5 forecast, MAE remains below 40 degrees for most sites, except for NAPS, RAPS, TAPS, and BARCV, where it reaches up to 60 degrees. Additionally, the results indicate that MAE tends to increase with longer lead times. These findings provide valuable insights into the temporal dynamics of wind speed across NPP sites, which are crucial for understanding and optimizing their operational strategies.

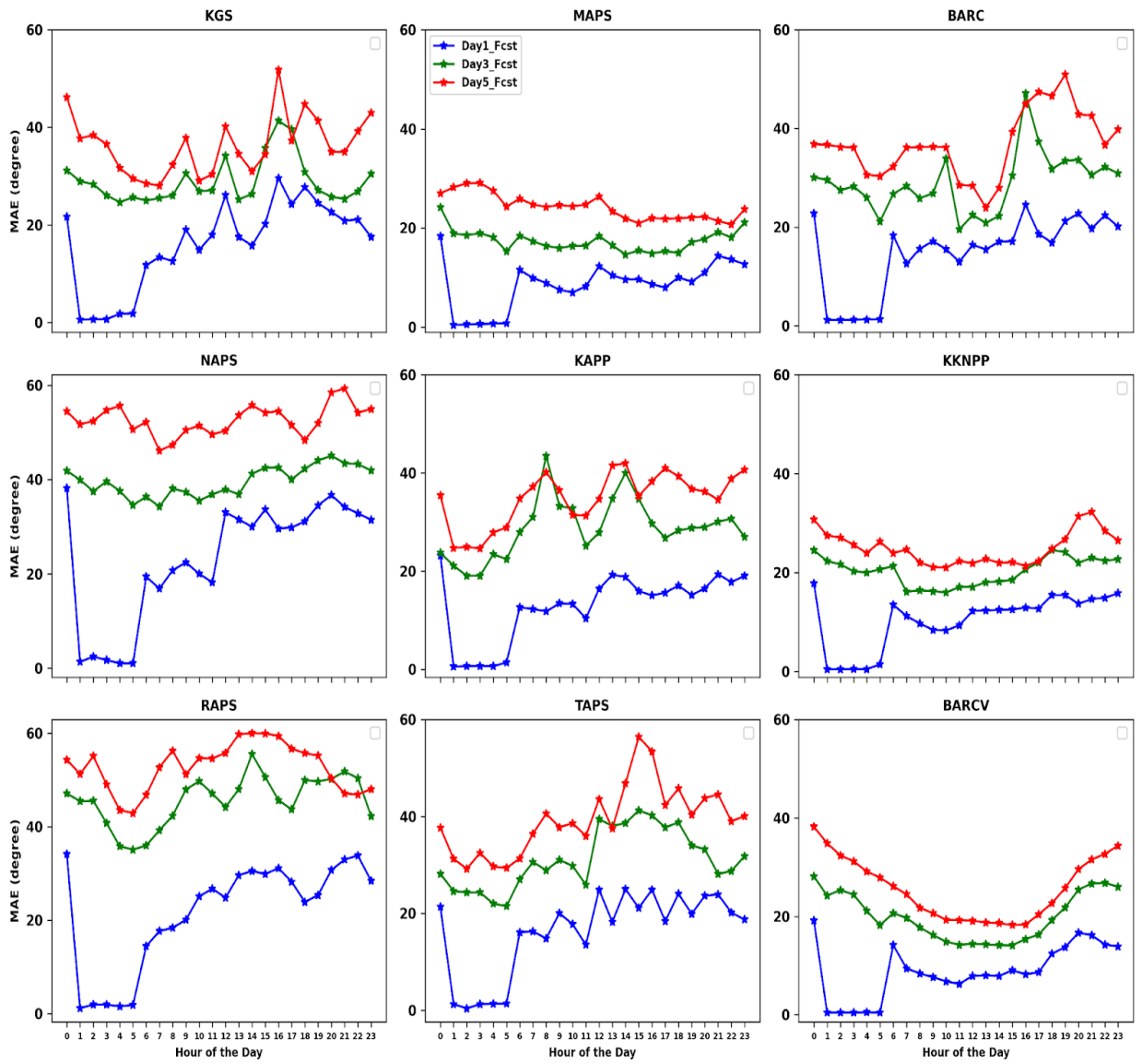

Figure 17: Diurnal variation in the MAE in forecast WD (against analysis) averaged over latitude-longitude for the nine NPCIL sites during October 2022-September2023 for lead times Day-1, 3 and 5.

4.2 Bias Correction

The analysis conducted in the model verification section strongly underscores the essential need for bias correction in forecasting. In this section we have attempted to reduce the model biases in forecast wind speed adopting the moving average bias correction techniques as suggested by (Cui et al., 2012; Singh et al., 2020)following the methodology described in section 3. The skill

assessment has been done in terms of mean bias (MB) in the wind speed. In Figure 18 the MB in the day 1 forecast from the model before and after bias-correction have been presented. The spatial variability of the error clearly shows that high wind regions such as Rajasthan and Gujarat where the errors in model forecasts are relatively higher are appreciably reduced. The bias correction also helps achieve lower errors over the NPP locations in particular RAPS and BARCV where the mean bias is relatively more. This concludes that a simple bias correction technique is helpful and efficient aligning the wind speed forecast to the model analysis.

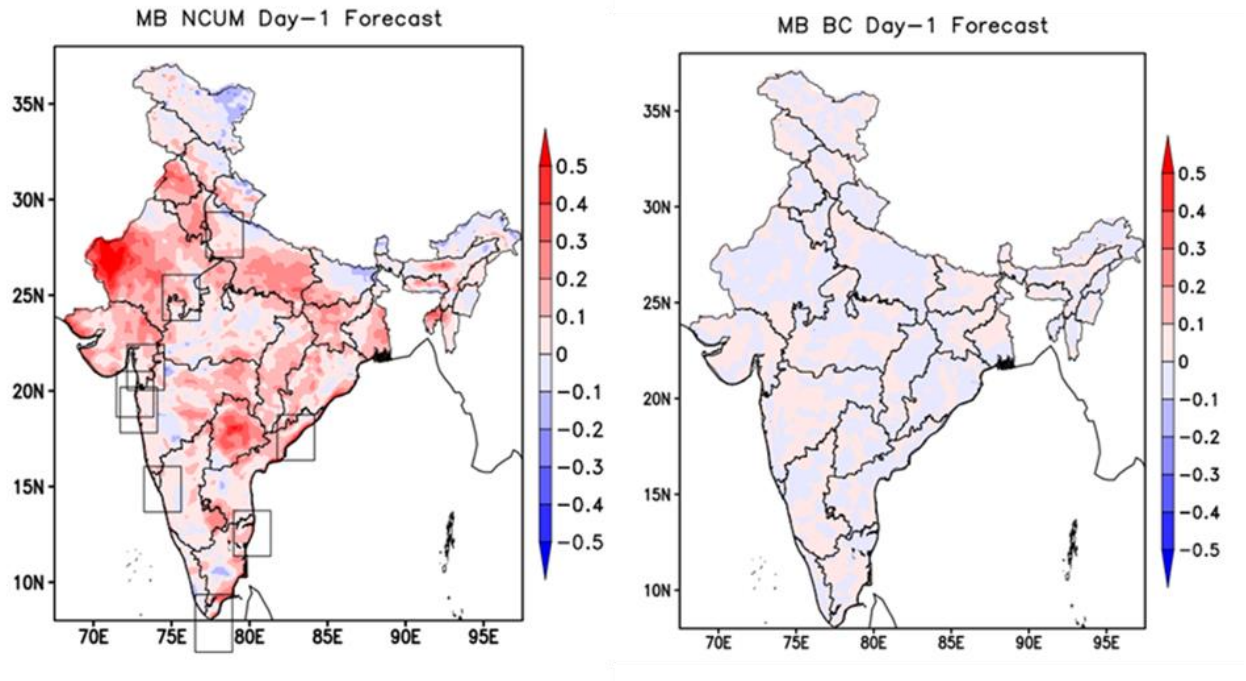

Figure 18: Comparison of Mean Bias Error (MBE) in Day 1 forecasts before and after bias correction, relative to model analysis, spanning the period from October 2022 to September 2023.

5. Conclusions

5.1 The spatial pattern of wind speed forecast is well captured till Day-5 forecast lead time. However, a discrepancy is seen in certain regions, notably over the seas in day 3 and day 5, where there is a tendency for overestimation that increases with lead time.

5.2 The model forecast accuracy in the first 24 hours (Day1) is reasonably good, with a Root Mean Square Error (RMSE) of less than 1.4 m/s for pan-India predictions. However, it decreases appreciably at higher lead times.

5.3 The wind speed data reveals notable seasonal patterns, with the highest mean wind speeds are observed during the summer months May to September, which can be characterized as the high wind season. Further, the study reveals that biases are particularly prominent during the same time of high WS.

5.4 The wind direction data also revealed significant seasonal patterns. Notably, the data indicated that the dominant wind direction during the summer months from May to September is south westerly direction. Further, the findings suggest that the Day-5 lead time forecast closely aligns with the model analysis, indicating a high level of accuracy in extended-range wind direction predictions.

5.5 The mean diurnal variation of hourly wind speed exhibits a consistent pattern with lower values during the early morning and a gradual increase through the day, peaking in the late afternoon.

5.6 The diurnal variability of wind direction varies across the NPP sites and model forecast are reasonably good even at higher lead times.

5.7 The scatter plots depict a high level of association between analysis and forecasted (Day 1) wind speed and direction, as seen by the high values of R^2 values exceeding 0.88 and 0.68 respectively for all sites. This robust correlation confirms the accuracy and reliability of the utilized forecasting model.

5.8 The Day-1 forecast distribution for each wind speed range closely matched the model analysis, indicating reliability in the forecasting approach.

5.9 The Day-1 wind speed forecasts compared to model analysis revealed consistently low MAE and RMSE values across all grids for all nine NPP sites, with each site exhibiting MAE values below 1 m/s and RMSE values below 1.3 m/s.

5.10 The annual variation in MAE in Day-1 wind speed forecasts compared to model analysis averaged over latitude-longitude for nine Nuclear Power Plant (NPP) sites revealed consistently low MAE below 0.5 m/s across most NPP sites, while Day-3 forecasts had an MAE below 1 m/s for all sites, while Day-5 forecasts reached up to 1.5 m/s for certain sites.

5.11 The annual variation in MAE in Day-1 wind direction forecasts compared to model analysis averaged over latitude-longitude for nine Nuclear Power Plant (NPP) sites revealed consistently low MAE below 25 degrees across most NPP sites, while Day-3 forecasts had an MAE below 70 degrees for all sites and for Day-5 forecasts MAE reached up to 95 degrees for certain sites.

5.12 The diurnal variation in MAE in Day-1 wind speed forecasts compared to model analysis averaged over latitude-longitude for nine Nuclear Power Plant (NPP) sites revealed consistently low MAE below 0.6m/s across most NPP sites, while Day-3 forecasts had an MAE below .9 m/s for all sites, while Day-5 forecasts reached up to 1.2 m/s for certain sites.

5.13 The diurnal variation in MAE in Day-1 wind direction forecasts compared to model analysis averaged over latitude-longitude for nine Nuclear Power Plant (NPP) sites revealed consistently low MAE below 20 degrees across most NPP sites, while Day-3 forecasts had an MAE below 40 degrees for all sites and for Day-5 forecasts MAE reached up to 60 degrees for certain sites.

5.14 Moving average bias correction technique significantly reduces errors in model forecasts, particularly in high wind regions like Rajasthan and Gujarat. Moreover, it leads to lower errors at NPP locations, especially RAPS and BARCV, where mean bias is more pronounced.

Limitations

The report thoroughly examines the performance of NCUM-G in forecasting wind speed and direction, highlighting the importance of implementing bias correction for accurate forecasts. We have introduced a straightforward approach and achieved satisfactory results in bias correcting wind speed. However, we have not addressed wind direction, which necessitates a distinct methodology due to its angular nature. Additionally, we plan to explore a more advanced technique

utilizing machine learning algorithms. Another approach we intend to explore involves bias correction of both the u and v components of winds, leading to improved forecasts of wind speed and direction crucial for the decision support system (DSS) during any nuclear emergency.

Authors Contribution: The report was conceptualized and supervised by Dr. Raghavendra Ashrit. Data Analysis, Methodology, and write up by Priya Singh. The report was reviewed and edited by Sushant Kumar.

References:

1. George, J.P., S. Indira Rani, A. Jayakumar, Saji Mohandas, Mallick, S., R. Rakhi, M. N. R. 512 Sreevathsa, E. N. Rajagopal, 2016. NCUM Data Assimilation System. 513 https://doi.org/10.13140/RG.2.1.3576.2167.

3. Rajagopal, E.N., Iyengar, G.R., George, J.P., dasgupta, munmun, Mohandas, S., Siddharth, 552 R., Gupta, A., Sharma, K., prasad, v. s., 2012. Implementation of the UM model based analysis-forecast system at NCMRWF (Technical), NMRF/TR/2/2012. 554 NCMRWF.

4. Kumar, S., Bushair, M.T., Buddhi, P., Lodh, A., Sharma, P., 2020. NCUM Global NWP 526 System: Version 6 (NCUM-G:V6) (Technical No. NMRF/TR/06/2020). NCMRWF.

5. Kumar, S., Jayakumar, A., Bushair, M.T., Buddhi, P., george, gibies, Lodh, A., Rani, S.I., 528 George, J.P., 2018. Implementation of New High Resolution NCUM Analysis-529 Forecast System in Mihir HPCS (Technical No. NMRF/TR/01/2018). NCMRWF.

6. Cheng, W.Y.Y., Steenburgh, W.J., 2005. Evaluation of Surface Sensible Weather Forecasts by the WRF and the Eta Models over the Western United States. Weather and Forecasting 20, 812–821. https://doi.org/10.1175/WAF885.

7. Coleman, R.F., Drake, J.F., McAtee, M.D., Belsma, L.O., 2010. Anthropogenic Moisture 503 Effects on WRF Summertime Surface Temperature and Mixing Ratio Forecast Skill In Southern

California. Weather and Forecasting 25, 1522–1535. 505 https://doi.org/10.1175/2010WAF2222384.1

8. Cui, B., Toth, Z., Zhu, Y., Hou, D., 2012. Bias Correction for Global Ensemble Forecast. Weather and Forecasting 27, 396–410. https://doi.org/10.1175/WAF-D-11-00011.1

9. Rajagopal E N, Iyengar G R, George J P, Gupta M D, Mohandas S, Siddharth R, Gupta A, Chourasia M, Prasad V S, Sharma A and Ashish K A 2012 Implementation of the UM model based analysis–forecast system at NCMRWF;NMRF/TR/2012, 45p.

10. Rani S I, Taylor R, Sharma P, Bushair M T, Jangid B P,George J P and Rajagopal E N 2019 Assimilation ofINSAT-3D imager water vapour clear sky brightness temperature in the NCMRWF's assimilation and forecast system; J. Earth Syst. Sci. 128 197, https://doi.org/10.1007/s12040-019-1230-6.

11. Kumar Sumit, M. T. Bushair, BuddhiPrakash J., AbhishekLodh, Priti Sharma, Gibies George, S. Indira Rani, John P. George, A. Jayakumar, Saji Mohandas, Sushant Kumar, Kuldeep Sharma, S. Karunasagar, and E. N. Rajagopal 2020: NCUM Global NWP System: Version 6 (NCUM-G:V6). NCMRWF Technical Report, NMRF/TR/06/2020.

12. Clayton, A. M., Lorenc, A. C. and D. M. Barker (2013): Operational implementation of a hybridensemble/4D-Var global data assimilation system at the Met Office. Q. J. R. Meteorol.Soc. 139: 1445-1461, doi:10.1002/qj.2054.
(2) (PDF) Implementation of New High Resolution NCUM Analysis-Forecast System in Mihir HPCS. Available from: https://www.researchgate.net/publication/327546230_Implementation_of_New_High_Resolution_NCUM_Analysis-Forecast_System_in_Mihir_HPCS.

13. University Corporation for Atmospheric Research Wind direction quick reference and accessed from: eol.ucar.edu/content/wind-direction-quick-reference.

14. Shrivastava R., et. al., (2015), Comparison of Two Prognostic Models WRF and TAPM for Short Range Forecasts for Kaiga India, International Journal of Earth and Atmospheric Science 2(3), 97 – 108.

16. Topics in Circular Statistics, S RaoJammalamadaka and A SenGupta, World Scientific Publishing Co. Pte. Ltd., 2021 5. Lee S-M, Fernando HJS (2004) Evaluation of meteorological models MM5 and HOTMAC using PAFEX-I data. J Appl Meteor 43:1133–1148 6.

17. Kalman, R.E., 1960. A New Approach to Linear Filtering and Prediction Problems. Journal of Basic Engineering 82, 35–45. https://doi.org/10.1115/1.3662552

18. Kumar, S., Ashrit, R., Mitra, A.K., Rai, S., 2022. Imdaa Regional Reanalysis: A New Source of Information for Wind and Solar Energy Resource Assessment Over India. SSRN Journal. https://doi.org/10.2139/ssrn.4312825

19.Singh, H., Dube, A., Kumar, S., Ashrit, R., 2020. Bias correction of maximum temperature forecasts over India during March–May 2017. J Earth Syst Sci 129, 13. https://doi.org/10.1007/s12040-019-1291-6.

20. K. Niranjan Kumar, Mohana S. Thota, Anumeha Dube, M.Venkatarami Reddy, Sumit Kumar and Raghavendra Ashrit .NCUM Global Model Verification: Monsoon (JJAS) 2022 (NMRF/VR/MAR/2023).

21. Kondapalli Niranjan Kumar, Raghavendra Ashrit, Sushant Kumar, C. J. Johny, Ashok Das, Ananda Das, B. P. Yadav and Ashish K. Mitra. Evaluation of Quantitative Precipitation Forecast Performance of NWP models in Indian River Basins 2023 (NMRF/RR/03/2023).